



Stabilizing Au(III) in supported-ionic-liquid-phase (SILP) catalyst using CuCl₂ via a redox mechanism



Jia Zhao ^{a,b,*}, Yi Yu ^a, Xiaolong Xu ^a, Shuxia Di ^a, Bolin Wang ^a, Hao Xu ^a, Jun Ni ^a, LingLing Guo ^a, Zhiyan Pan ^b, Xiaonian Li ^{a,**}

^a Industrial Catalysis Institute of Zhejiang University of Technology, State Key Laboratory Breeding Base of Green Chemistry-Synthesis Technology, Hangzhou, 310014, People's Republic of China

^b Department of Environmental Engineering, Zhejiang University of Technology, Hangzhou, 310014, People's Republic of China

ARTICLE INFO

Article history:

Received 11 October 2016

Received in revised form 7 December 2016

Accepted 11 January 2017

Available online 12 January 2017

Keywords:

Au catalysis

Supported ionic liquid phase

Acetylene hydrochlorination

CuCl₂

Reoxidation

ABSTRACT

High-valent Au(III) complexes have attracted much attention as catalysts in many reactions. Nevertheless Au(III) catalysts suffer from instability of the oxidized metal complexes during preparation and use. Herein, we demonstrated that Au(III) catalysts can be stabilized against reduction to metallic Au⁰ by modifying supported-ionic-liquid-phase-stabilized Au(III) catalyst with CuCl₂. It was found that the reduced Au⁰ could be re-oxidized in situ to Au³⁺ species by CuCl₂ during the reaction and further stabilized by the electron transfer from Cu to these active species. When evaluated in the acetylene hydrochlorination reaction, the Au-Cu-IL/AC catalyst displayed an excellent specific activity with the turnover frequency (TOF) as high as 168.5 h⁻¹ and more than 99.8% selectivity for the product, vinyl chloride (VCM). Furthermore, the Au-Cu-IL/AC catalyst demonstrated a stable catalytic performance with a negligible loss of C₂H₂ conversion after 500 h under typical industrial reaction conditions for acetylene hydrochlorination. Therefore, the findings of this work provide an efficient approach for designing stable high-valent metals for long-term operation, and also pave the way for the application of Au-Cu-IL/AC catalyst in industrial VCM production.

© 2017 Elsevier B.V. All rights reserved.

1. Introduction

Vinyl chloride is a monomer (VCM) for the industrially important polymer, polyvinyl chloride (PVC). The manufacture of VCM is carried out either via an oxychlorination reaction using ethylene as a substrate or via hydrochlorination of acetylene on an industrial scale [1]. As the latter method is less expensive compared to oxychlorination reaction based on petroleum, VCM is primarily manufactured via hydrochlorination of acetylene in many developing countries that are rich in coal reserves [2]. Commercial processes for industrial VCM production use mercuric chloride (HgCl₂) supported on activated carbon (AC) as catalyst [3]. However, the main problem concerning hydrochlorination of acetylene using conventional HgCl₂ catalysts is that they undergo severe deactivation. Moreover, due to the volatility of the toxic mercuric component, it can be dispersed into the environment and pose a serious threat to both human and animal health. At present about

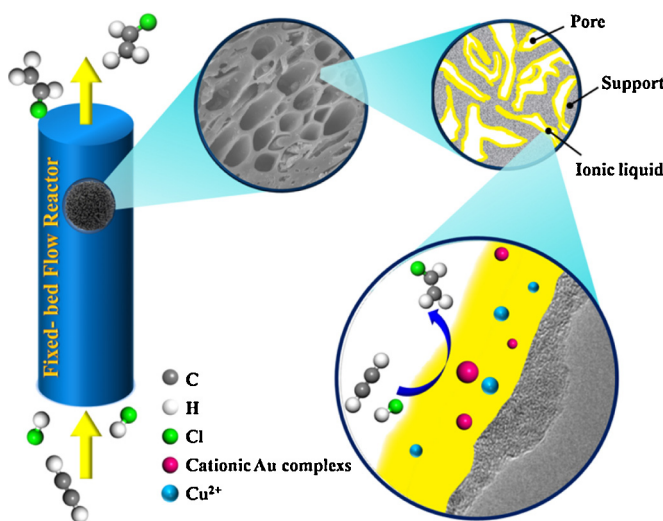
600–1000 tons of HgCl₂ per annum are lost from the mercury catalyst [4]. Thus, for an industrial-scale production, the use of mercury-free catalyst as replacement for the toxic HgCl₂ is highly necessary.

In the past two decades, many efforts have been devoted to the development of more efficient and stable non-mercuric catalytic systems that are suitable for practical use [5–16]. Different transition metals, non-precious metals, and even nonmetallic materials have been evaluated and found to catalyze the reaction in the following order of decreasing activity: gold > other precious metals > non-precious metals > nonmetallic materials. Despite cationic Au species (Au³⁺ and Au⁺) being presented in the literature as the most promising alternative for HgCl₂, their high cost and instability in the cationic form during acetylene hydrochlorination restrict its practical application [17,18]. Therefore, the primary objective in the field is to prepare a stable, yet catalytically active, low-loading Au-based catalyst which meets the above criteria. Modification of Au-based catalysts by adding a second metal component [19–25] or doping carbon supports with heteroatoms [26–28] have been commonly investigated to stabilize cationic Au active species. However, these strategies to prepare Au-based catalysts still suffer from several drawbacks, as the modified Au-based catalysts have limited lifetime of activity due to the facile reduction of cationic Au species

* Corresponding author at: Industrial Catalysis Institute of Zhejiang University of Technology, State Key Laboratory Breeding Base of Green Chemistry-Synthesis Technology, Hangzhou, 310014, People's Republic of China.

** Corresponding author.

E-mail addresses: jiazhao@zjut.edu.cn (J. Zhao), xnli@zjut.edu.cn (X. Li).



Scheme 1. Schematic view of a supported ionic liquid phase (SILP) catalyst system.

to metallic Au^0 . Moreover, Au could not be effectively dispersed onto the AC supports both during the preparation and reaction process.

Recently, we have described a highly active supported-ionic-liquid-phase (SILP) catalyst for the gas-phase hydrochlorination of acetylene in a fixed-bed reactor [29]. Within this system, the IL film not only provides a solvent environment for the highly dispersed metal active center complex, but also dissolves the reaction substrates to facilitate their access to the active sites [30–35]. More importantly, the presence of ILs can effectively stabilize the oxidized metal complex and prevent the formation of agglomerates [36,37]. The activity of Au-IL/AC at 180°C and 370 h^{-1} led to turnover frequencies (TOF) as high as 79.2 h^{-1} with $>99.8\%$ selectivity for VCM [29]. Thus, the basis for retention of a highly active and selective catalyst is provided. However, these systems were also deactivated after prolonged use due to the Au^{3+} species being reduced to metallic Au^0 . Thus, the problem of instability of Au-based catalysts has not yet been fully resolved and the development of efficient and stable Au-based catalysts continues to pose a research challenge.

The present work builds on our earlier study with the Au-IL/AC catalyst, with the added dimension of exploring the CuCl_2 -modified Au-IL/AC catalyst (Scheme 1). Indeed, it has been reported that active Au-based catalysts acquired specific and sometimes unexpected properties when modified with Cu [38–43]. A few papers have already been published, in which AuCl_3 and CuCl_2 were combined to produce acetylene hydrochlorination catalysts [21,44–47]. However, in these systems, CuCl_2 is only deemed to function as an electron promoter. This is in contrast with our current catalyst, in which CuCl_2 is present in Au-Cu-IL/AC catalyst to not only increase the electron density of cationic Au active species but also to in situ re-oxidize the reduced Au^0 species back to cationic Au species. In this work, the activity and stability of the Au-Cu-IL/AC catalyst were thoroughly evaluated in the gas-phase hydrochlorination of acetylene. The encouraging preliminary results of this work can contribute to the development of highly active, stable and low-cost Au-based catalysts for the acetylene hydrochlorination reaction.

2. Experimental

2.1. Chemicals

Activated carbon (Norit ROX 0.8, surface area of $1100\text{--}1200\text{ m}^2/\text{g}$, pore volume of $0.63\text{ cm}^3/\text{g}$, density of 400 g/L ,

max. 0.5 mm in diameter, $1\text{--}5\text{ mm}$ in length) were used as the catalyst support. $\text{HAuCl}_4 \cdot 4\text{H}_2\text{O}$ (Au content $\geq 49\%$) was supplied by Sigma-Aldrich. $\text{CuCl}_2 \cdot 2\text{H}_2\text{O}$ ($\text{CuCl}_2 \cdot 2\text{H}_2\text{O}$ content $\geq 99.9\%$) was supplied by Aladdin Industrial Corporation (Shanghai, China). The C_2H_2 gas (purity $> 98.0\%$) was treated via passing through a $\text{K}_2\text{Cr}_2\text{O}_7$ solution to get rid of H_2S and PH_3 , and then a H_2SO_4 solution to get rid of H_2O . The HCl gas (purity $> 99.99\%$) was used without further purification. Ionic liquids (IL), 1-propyl-3-methylimidazolium chloride ([Prmim]Cl, purity $> 99\%$) was purchased from Lanzhou Greenchem ILS, LICP, CAS. (Lanzhou, China), and used without further treatment.

2.2. Catalyst preparation

Briefly, the catalyst preparation involved dissolving the required amounts of $\text{HAuCl}_4 \cdot 4\text{H}_2\text{O}$ and $\text{CuCl}_2 \cdot 2\text{H}_2\text{O}$ precursors in IL, followed by stirring at room temperature for 1 h in order to allow a perfect homogenization of the resulting Au-Cu-IL complex. The procedure to support the Au-Cu-IL complex on the AC materials is as follows: about 5 g of the AC were degassed in vacuum at 150°C for 1 h; after cooling, the desired amount of Au-Cu-IL complex, mixed with a minimal amount of deionized water, was added to the outgassed AC and stirring for 0.5 h. Then, the obtained heterogeneous catalyst was dried at 110°C in a vacuum oven for 12 h. The same process was also employed to synthesize the non-promoted Au-IL/AC, Cu-IL/AC and IL/AC for comparison. Au loading in all the Au-SILP catalysts was fixed at 0.1 wt%. All supported Au-SILP complex catalysts contained 10 wt% IL. Monometallic Au/AC, 1Au/AC and 10Hg/AC catalysts were prepared using incipient wetness impregnation technique as reported before [24].

2.3. Characterization of catalysts

The porosity properties of the materials were obtained from N_2 adsorption-desorption isotherms using Micromeritics ASAP 2000 system. Before the measurement, the samples were first outgassed at 150°C for 2 h. The specific surface areas and the pore size distribution were calculated based on the BET method. The metal contents within the catalysts were determined by ICP-MS method (PerkinElmer Elan DRC-e). X-ray diffraction (XRD) analysis were conducted on a PANalytical X'Pert diffractometer with $\text{Cu K}\alpha$ radiation ($\lambda = 0.1541\text{ nm}$) operating at a voltage of 40 kV and a current of 40 mA . XRD profiles were collected between $2\theta = 20\text{--}80^\circ$ with a step width of 0.05° . Morphology and microstructures of the catalysts are characterized by transmission electron microscopy (TEM). The powder samples of the catalysts were ultrasonically dispersed in ethanol and mounted onto Ni grids covered with holey carbon film (Beijing Zhongjingkeyi Technology Co., Ltd.). A Tecnai G2 F30 S-Twin electron microscope, operating at 300 kV and equipped with EDX analyzer system were used for TEM observation. X-ray photoelectron spectroscopy (XPS) analysis was performed with a Kratos AXIS Ultra DLD apparatus, equipped with monochromated aluminum X-ray source, a charge neutralizer, and a hemispherical electron energy analyzer. The pressure in the sample analysis chamber was lower than $6 \times 10^{-9}\text{ Torr}$ during data acquisition. The spectra were analyzed using the XPSPEAK41 software pack and corrected for charging using $\text{C } 1\text{s}$ binding energy (BE) as the reference at 284.8 eV . Thermogravimetric analysis (TGA) were recorded using a NETZSCH STA 449C Jupiter instrument between 30 and 600°C , with a heating rate $10^\circ\text{C}/\text{min}$. Temperature-programmed desorption (TPD) experiments were performed in a tubular quartz reactor. The samples (about 75 mg) were first treated in situ at 180°C for 0.5 h using pure HCl and then cooled to room temperature in the same atmosphere. The sample was swept with pure Ar at a flow rate of $30\text{ mL}/\text{min}$ for 1 h to remove physisorbed and/or weakly bound species. TPD was performed by heating the sample from room tem-

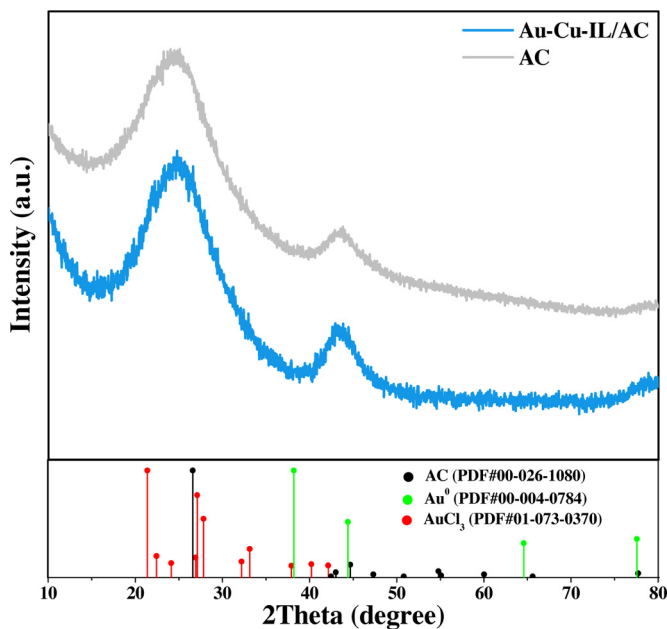


Fig. 1. XRD patterns of the AC support and fresh Au-Cu-IL/AC catalyst.

perature to 500 °C at a ramp rate of 10 °C/min in pure Ar, and the TPD spectra were recorded by a quadrupole mass spectrometer (QMS 200 Omnistar).

2.4. Catalytic activity and selectivity evaluations

All acetylene hydrochlorination experiments were carried out in a continuous fixed bed reactor consisted of a quartz reaction

tube (10 mm diameter, 380 mm length). Catalyst samples were evaluated as follows: 0.2 g of each sample was loaded into the quartz tube, and reacted under the flow of C₂H₂ (5 mL/min) and HCl (6 mL/min) at 180 °C. For stable operation, both C₂H₂ and HCl gas flows were dosed by a digital mass flow controller (D07-19B). The pressures of both C₂H₂ and HCl gas were in the range of 1.0–1.1 bar for safety reasons. Reaction temperature was controlled by a thermocouple placed inside the catalytic fixed bed using AI-708P temperature controller (Xiamen Yudian Automation Technology CO., LTD.). Prior to heating, the reactor was flushed three times with N₂ gas to remove air in the reaction tube. When reaching the desired reaction temperature, HCl gas was fed into the reactor to activate the catalyst for 0.5 h. The remaining gas flow was led to a gas chromatograph (Fuli GC9790) for quantitative analysis. The GC was equipped with a Porapak Q packed column with adjacent a flame ionization detector (FID). By means of an automated software, a GC injection was performed at least every half an hour.

3. Results and discussion

3.1. Characterization of the as-prepared Au-Cu-IL/AC catalyst

The synthetic procedure for preparing the Au-Cu-IL/AC catalyst was based on a modified strategy that was previously reported for the synthesis of SILP system [48]. After preparation, the catalyst was characterized by XRD, TEM and XPS analyses. Fig. 1 shows the obtained XRD of the bare AC support and the Au-Cu-IL/AC catalyst, and only the diffraction lines corresponding to the AC (PDF 00-026-1080) support are observed. This is likely because Au and Cu are possibly too well dispersed over the catalyst material to show up as crystalline phases or the content of Au and Cu could be below the detection limit of the XRD technique. The STEM images and the energy dispersive spectroscopy (EDS) spectrum indicate

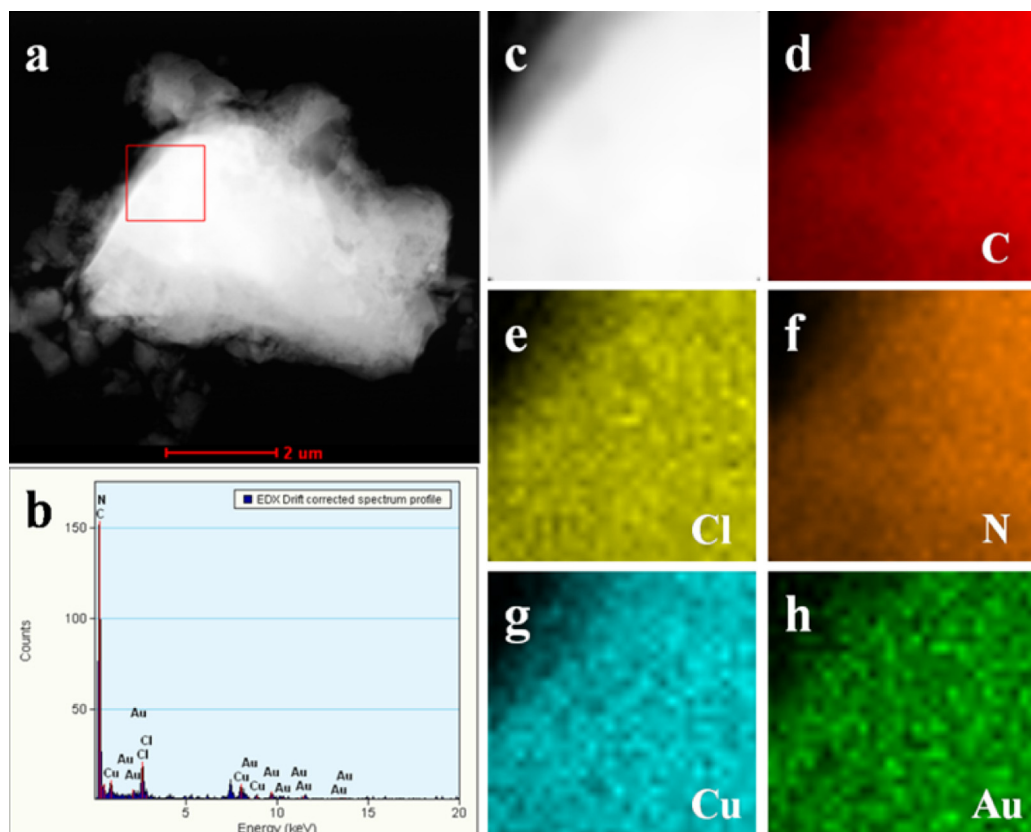


Fig. 2. (a) STEM image, (b) EDX analysis and (c–h) elemental mapping images of the fresh Au-Cu-IL/AC catalyst.

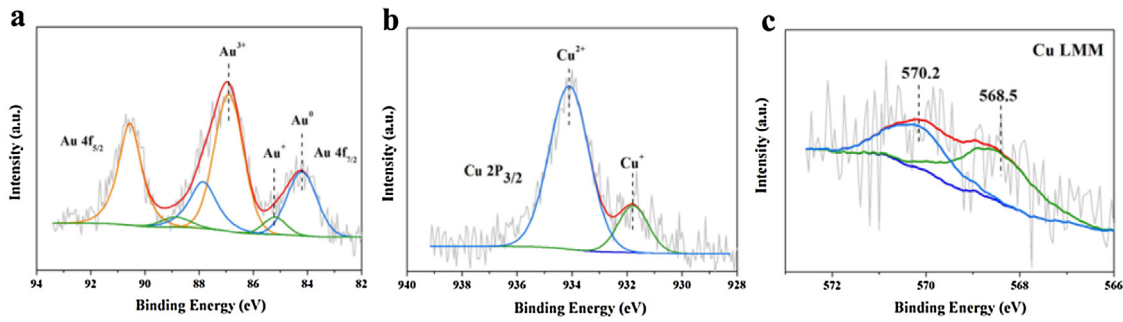


Fig. 3. (a) Au 4f, Cu 2p core level and (c) Cu LMM Auger spectra of fresh Au-Cu-IL/AC catalyst.

the presence of certain amounts of Au and Cu species as well as heteroatoms, such as N and Cl (Fig. 2a–b). However, no Au or Cu particles were observed, indicating a high level of dispersion. It is also likely that most of the metal compounds that are homogeneously distributed on the surface of the catalyst materials, existed as non-crystalline species, which was confirmed by elemental mapping using STEM/EDS spectroscopy (Fig. 2c–h). These features are consistent with the XRD results mentioned above.

Fig. 3 shows the XPS analysis of Au 4f and Cu 2p region for the fresh Au-Cu-IL/AC catalyst. As shown in Fig. 3a, the Au-Cu-IL/AC showed three Au states characterized by Au 4f_{7/2} binding energy (BE) of 84.2, 85.2 and 86.9 eV, respectively (Fig. 3a). The Au 4f_{7/2} energy of 86.9 eV is very similar to the energy of Au state in the starting reagent, AuCl₃ complex having the Cl ions as the ligands [49]. The peaks at 85.2 eV can be attributed to the low-valent Au⁺ species, which are reported to have a lower BE than Au³⁺ species. The third Au state with the lowest BE of 84.2 eV indicates the presence of metallic Au⁰ species. The ratio of Au³⁺, Au⁺ and Au⁰ is

62.2:7.3:30.5. Previous literature confirmed that Au exists in the predominantly metallic Au⁰ state in Au/AC [52]. The high proportion of cationic Au species (69.5%) can be explained by the fact that the Au³⁺ and Au⁺ species are dissolved and stabilized in the IL layer. The strong stability of the cationic Au species facilitates their good performance in hydrochlorination thereafter. In addition, the binding energy of Au⁰ species is 0.2 eV higher than that of the standard values (84.0 eV), which could be due to the electron transfer from Cu to Au atoms.

Fig. 3b shows the XPS spectra of Cu 2p_{3/2} core level for Au-Cu-IL/AC. The peaks were also deconvoluted for different Cu species in the sample [53,54]. The peak at 934.1 eV is assigned to Cu²⁺ species. The lower BE peak at 931.7 eV suggests the presence of Cu⁺ or Cu⁰ species. As the BE of Cu 2p_{3/2} does not allow us to make a distinction between Cu⁺ and Cu⁰, Auger Cu LMM spectra (Fig. 3c) were obtained to identify the existence of Cu⁺ at BE 570.2 eV. Considering that the presence of ionic liquid in the Au-Cu-IL/AC catalyst prevents the direct interaction of the Au³⁺ and Cu²⁺ species with the carbon

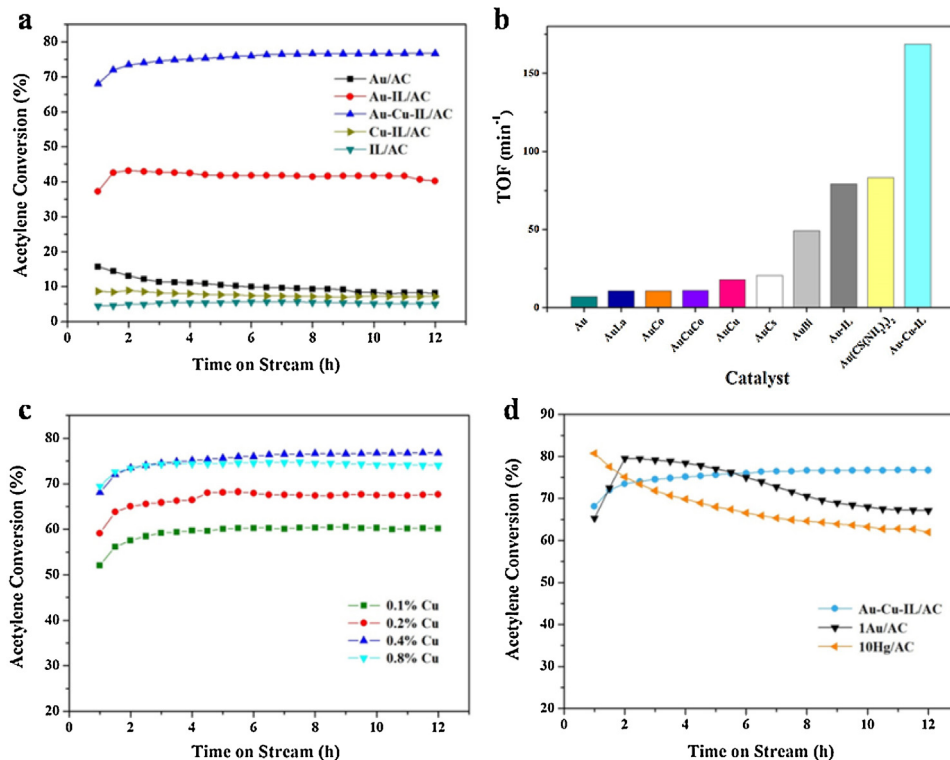


Fig. 4. Evaluation of acetylene hydrochlorination performances of Au-Cu-IL/AC catalysts. (a) Conversion of acetylene to VCM in acetylene hydrochlorination over Au-Cu-IL/AC, Au-IL/AC, Au/AC, Cu-IL/AC and IL/AC catalysts. (b) The TOF value for the different Au-based catalysts reported in literatures [4,20–24,29,47,50]. (c) Catalytic activity of Au-Cu-IL/AC as a function of the amount of Cu loading. (d) The comparison of the reactivity and stability of Au-Cu-IL/AC, 1Au/AC (Au = 1.0 wt%) and 10Hg/AC (Hg loading = 10.0 wt%) catalysts. Reaction conditions: T = 180 °C, C₂H₂ gas hourly space velocity (GHSV) = 740 h⁻¹, feed volume ratio V(HCl)/V(C₂H₂) = 1.2:1.

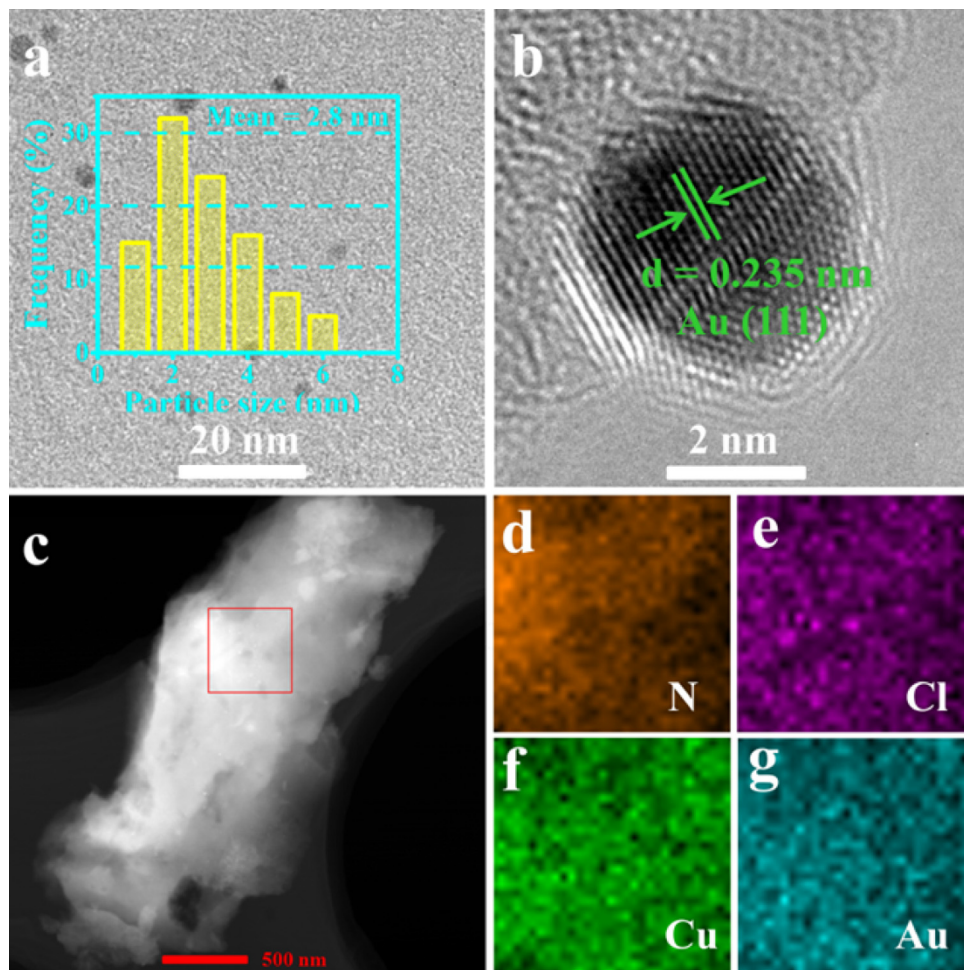


Fig. 5. (a) TEM image and corresponding size distribution of the used Au-IL/AC sample. (b) HRTEM image of the used Au-IL/AC. (c) STEM image and (d-g) corresponding elemental mapping images of the used Au-Cu-IL/AC sample.

surface and the fact that XPS analysis may result in the reduction of metal ions, it is very likely that the low valence and/or metallic state formed in the Au-Cu-IL/AC sample is due to the prolonged exposure of Au^{3+} and Cu^{2+} species to X-rays during the XPS analysis [50,51].

3.2. Catalytic properties for the hydrochlorination of acetylene

For continuous-flow catalysis, the catalytic performance of the prepared materials was tested in a lab-scale fixed-bed reactor at 180 °C and with a C_2H_2 gas hourly space velocity (GHSV) of 740 h⁻¹. Fig. 4a shows the acetylene hydrochlorination catalytic properties of both the Au-SILP catalysts and the respective Cu-IL/AC, IL/AC and Au/AC materials for comparison. Au/AC can catalyze the acetylene hydrochlorination reaction, with a conversion of 15.7% observed after 12 h reaction at 180 °C. In comparison, Au-IL/AC exhibited a higher conversion of 43.2% under the same reaction conditions. Of all the tested materials, Au-Cu-IL/AC displayed the highest catalytic activity. When the reaction reached the steady state, Au-Cu-IL/AC showed superior activity with more than 76.7% acetylene conversion (in these experiments, 76.7% conversion corresponds to a TOF of 168.5 h⁻¹ and space-time yield (STY) for VCM of 3.2 kg/(kg Cat·h)). These results clearly indicate that the efficiency of the Au-IL/AC catalyst for hydrochlorination of acetylene has been greatly improved after addition of CuCl_2 . It should be noted that acetylene conversion is only about 8.9 and 5.7% with Cu-IL/AC and IL/AC alone, respectively (Fig. 4a), indicating a negligible contribution from the IL and CuCl_2 to the high catalytic activity of Au-Cu-IL/AC catalyst.

When compared with other typical Au-based catalysts reported in previous works (Fig. 4b), one can say that the Au-Cu-IL/AC is one of the most efficient catalytic materials based on its relatively high TOF value. Moreover, the non-promoted Au-IL/AC exhibits slow deactivation after reaching the maximum activity (Fig. 4a). The acetylene conversion decreased by about 3.2% from the initial 43.2%. In comparison, the conversion over the Au-Cu-IL/AC catalyst does not drop, verifying that the catalysts are not deactivated. In fact, for the Au-Cu-IL/AC catalysts, the C_2H_2 conversion even increases from 68.1 to 76.8%. It should be noted that all the Au-based catalysts showed more than 99.8% selectivity towards VCM, and only trace amounts (<0.2%) of byproducts such as 1,2-dichlorethane and chlorinated oligomers can be observed.

Systematic evaluations were also performed by varying the amount of CuCl_2 and the results are shown in Fig. 4c. As can be seen, the loading of CuCl_2 affects the catalytic performance significantly. While increasing the loading of CuCl_2 from 0.1 to 0.4 wt%, the maximum acetylene conversion increases from 60.4 to 76.8%. After this point, a further increase in the amount of CuCl_2 from 0.4 to 0.8 wt% does not improve the activity and in fact, starts to lower the activity. The decrease in activity with the increase in the amount of CuCl_2 indicates that CuCl_2 may have some interaction with the AuCl_3 catalyst. The best results were obtained when 0.4 wt% CuCl_2 was used with the molar ratios of IL, Au and Cu being 123:1:12.

Furthermore, the activity of this low-loading Au-Cu-IL/AC system was superior to those of the commercial acetylene hydrochlorination catalysts 10Hg/AC (10 wt% Hg) and 1Au/AC

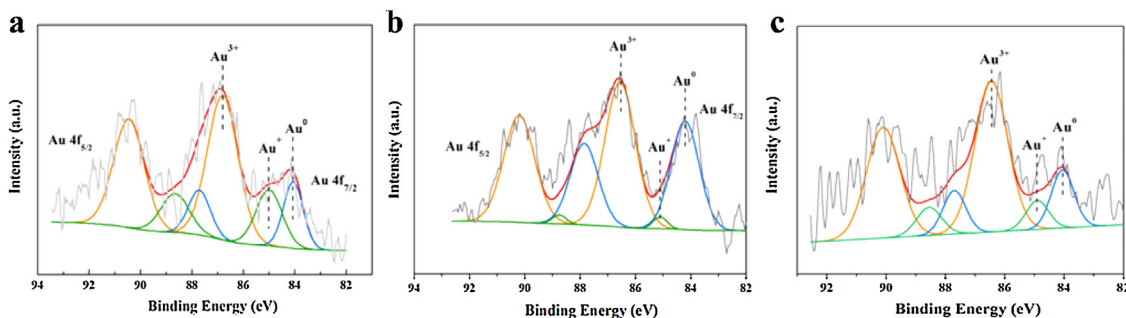


Fig. 6. Au 4f XPS spectra of (a) fresh Au-IL/AC, (b) used Au-IL/AC and (c) used Au-Cu-IL/AC catalysts.

Table 1
Au and Cu content in the fresh and used Au-IL/AC and Au-Cu-IL/AC based on the ICP analysis.

catalysts	Nominal loading (wt%)		Results of ICP (wt%)	
	Au	Cu	Au	Cu
Fresh Au-IL/AC	0.100	/	0.106	/
Used Au-IL/AC	0.100	/	0.104	/
Fresh Au-Cu-IL/AC	0.100	0.400	0.102	0.412
Used Au-Cu-IL/AC	0.100	0.400	0.997	0.405

(1 wt% Au) under the same conditions (Fig. 4d). As we know, the commercial catalyst has been optimized against the variation of reaction conditions. Nevertheless, this direct comparison underlines the enormous potential of the SILP technology for acetylene hydrochlorination catalysis. Even compared with the most active Au catalyst (1Au/AC), the Au-Cu-IL/AC has a comparable activity and higher stability, further highlighting its excellent catalytic performance.

3.3. Influence of CuCl₂ on the Au-SILP catalyst

3.3.1. Catalyst sintering

Characterizations of Au-SILP catalysts were conducted using various analysis techniques to obtain information on the surface morphology and valence states after the reaction. It is well-known that the metal nanoparticles (NPs) tend to grow or aggregate, which may lead to a significant decrease of catalytic activity. As the structure of catalyst can be changed during the reaction, TEM analysis was performed to evaluate whether the NPs sintered during the reaction. Fig. 5 shows the TEM and STEM images of the used Au-SILP catalysts. For Au-IL/AC (Fig. 5a), TEM images revealed the presence of a certain amount of metal NPs with sizes in the range of 1–6 nm. The average size is about 2.8 nm, which is markedly different when compared to the fresh catalyst (no Au or Cu particles could be observed). The HR-TEM images show that the crystal lattice spacing is 0.235 nm, which is indicative of the Au (111) plane (Fig. 5b). This result suggested that the non-promoted Au-IL/AC is not resistant to agglomeration or sintering during the reaction. Interestingly, in the Au-Cu-IL/AC system, the Au NPs could not be observed even after reacting for 12 h (Fig. 5c). STEM mapping indicated that the Au, Cu, N and Cl elements were still well dispersed and well sep-

arated throughout the entire supporting material (Fig. 5d–g). This result indicates that there was no sintering of Au NPs during the reaction, and this stabilization was almost certainly a result of the presence of CuCl₂.

3.3.2. Valence change

As previously mentioned, the catalyst deactivation is mainly attributed to the reduction of cationic Au species (Au⁺ and/or Au³⁺) to metallic Au⁰. Thus, further characterization of the mono- and bimetallic Au-SILP systems was achieved using XPS measurements to verify the change in the valence states of the Au-based catalysts after the reaction, and the results are presented in Fig. 6. Au species of the fresh Au-IL/AC catalyst were quantified based on the XPS spectra of Au 4f_{7/2}, and the three Au species, Au⁰, Au⁺ and Au³⁺, were identified (Fig. 6a). Compared with the fresh catalyst, the proportion of surface cationic species (Au⁺ and Au³⁺) decreased from 69.5 to 57.7% for the used Au-IL/AC catalyst (Fig. 6b). This is because the surface cationic Au species are reduced to metallic Au⁰, indicating the poor stability of cationic Au species in the non-promoted Au-IL/AC. In sharp contrast, XPS confirms that the content of Au³⁺ species increased significantly (80.9%) while the content of metallic Au⁰ decreased (19.1%) in the bimetallic Au-Cu-IL/AC catalysts after the reaction (Fig. 6c). The result indicates that the key role of Cu²⁺ on stabilizing the Au³⁺ may be played via re-oxidizing the reduced Au⁰ to cationic Au species under the reaction conditions, and this is explored in subsequent sections.

3.3.3. Active component leaching

To determine the amounts of fresh and used Au-SILP catalysts, ICP-MS analysis was conducted (Table 1). The ICP-MS results confirmed that Au contents in both the used Au-IL/AC and Au-Cu-IL/AC catalysts were consistent with the nominal amount of Au impregnated onto the AC support (detection limit ca. 100 ppb). Thus, an end-of-run ICP analysis of the fresh and used Au-SILP catalysts revealed that no metal leaching occurred.

3.4. Stability of IL

Specific attention was also paid to the stability of supported IL for the Au-Cu-IL/AC catalyst. The XPS results allow estimation of the relative amounts of N on the catalyst surface, as shown in Fig. 8. The survey scan spectra of the fresh and used Au-Cu-IL/AC confirmed

Table 2

The atomic ratio (calculation from XPS analysis) and surface area of the fresh and used Au-Cu-IL/AC.

sample	C	O	N	Cl	N/C	Surface area	Pore volume
						(m ² g ⁻¹)	(cm ³ g ⁻¹)
Fresh Au-Cu-IL/AC	82.55	8.34	3.20	5.91	3.88	753	0.42
Used Au-Cu-IL/AC	82.49	7.95	3.06	6.50	3.71	781	0.42

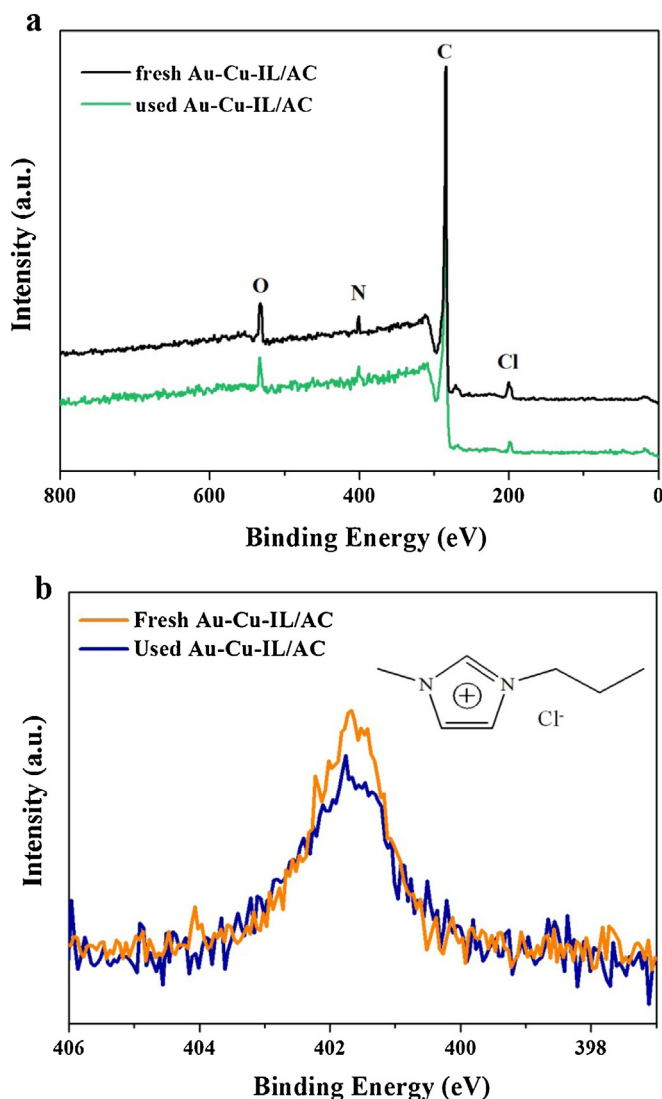


Fig. 7. (a) XPS sweep scan and corresponding high-resolution spectra of (b) N 1s. All spectra were normalized to the same photon flux of the X-ray source and shifted.

the presence of N atoms (Fig. 7a), which must originate from the [Prmim]Cl IL because it is the only N source in the catalyst system. Fig. 7b shows the XPS spectra of N 1s region for the fresh and used Au-Cu-IL/AC. As can be seen, the two nearly equivalent imidazolium N atoms show a single peak at 401.8 eV. The relative N/C atomic ratio was 3.88% in the fresh catalyst (Table 2). After the reaction, no drastic changes in the ratio of surface N atoms to carbon were observed (3.71%). Thus, XPS analysis showed that there was negligible loss of [Prmim]Cl IL because no notable change in the N/C atomic ratio could be observed after the reaction. This is also in good agreement with the fact that there is no drastic change in BET surface area of Au-Cu-IL/AC, as revealed by N_2 sorption isotherms (Table 2). TGA analysis revealed that the decomposition of [Prmim]Cl started at around 280 °C (Fig. 8), about 100 °C higher than the reaction temperature employed. Moreover, TGA shows that the decomposition of [Prmim]Cl within the AC support started at around 300 °C, about 20 °C higher than that of the corresponding IL in the open space, which may be because the static-assisted CH- π interaction between ILs and graphitic support modifies their thermal behavior [55]. Considering the non-volatility of [Prmim]Cl IL and the fact that a negligible amount of the IL thermal decomposition and/or leaving was found, we can conclude that the IL was completely trapped in the AC support. Thus, the [Prmim]Cl merits

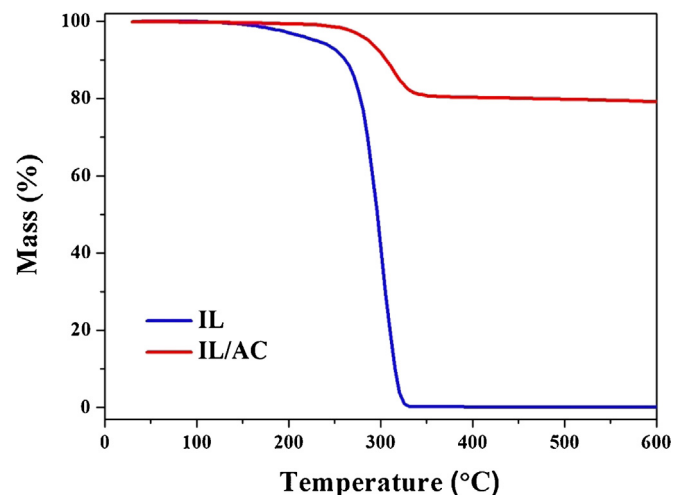


Fig. 8. TGA curves of pure IL and IL/AC in N_2 with a heating rate of 10 °C/min.

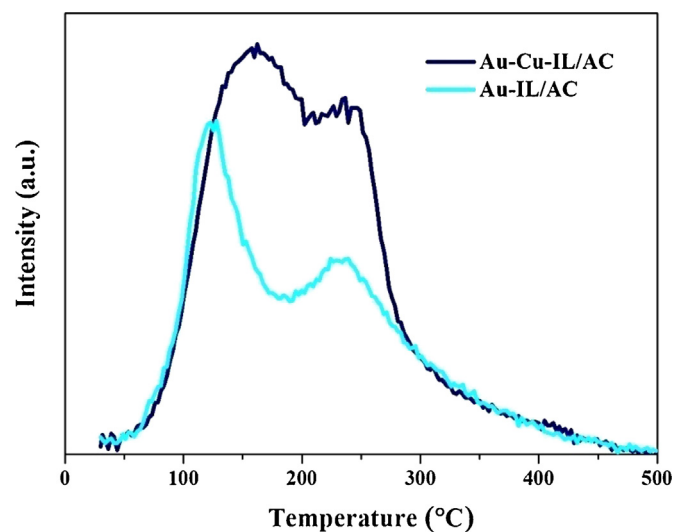
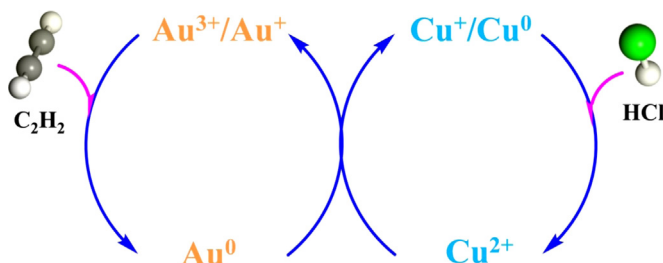


Fig. 9. TPD profiles of HCl on Au-IL/AC and Au-Cu-IL/AC catalysts.

further evaluation due to its excellent thermal stability under the reaction conditions.

3.5. Possible mechanism

Recently, many literatures reported that $CuCl_2$ is used as a promoter to improve the catalytic activity and prolong the life of Au catalyst in the gas-phase acetylene hydrochlorination [44–47]. In the bimetallic Au-Cu/C catalyst, $CuCl_2$ serves as an electron donor and $AuCl_3$ serves as an electron receptor. The electron density of $AuCl_3$ is increased, due to which hydrogen chloride (HCl) molecules are easily adsorbed on it. To investigate this effect in our Cu-promoted Au-IL/AC catalysts, HCl-TPD analysis was carried out to characterize the active sites for the HCl adsorption. As shown in Fig. 9, the Au-IL/AC and Au-Cu-IL/AC catalysts presented a band between 60 and 450 °C, which was characteristic of HCl desorption. However, the areas of the HCl-TPD peaks for the Au-Cu-IL/AC catalyst were much larger than for the Au-IL/AC catalyst. This suggested an increase in chemisorbed HCl on Au-Cu-IL/AC compared to Au-IL/AC. The favorable adsorption of HCl on Au-Cu-IL/AC is likely because electron transfer occurred from Cu to Au, which enhanced the electron-donating ability of Au center and allowed the catalyst to combine with more HCl. It has been reported that when HCl and C_2H_2 molecules were co-adsorbed on $AuCl_3$, C_2H_2 was co-



Scheme 2. Schematic representation of the proposed oxidative mechanism for Au^0 by Cu^{2+} over the Au-Cu-IL/AC catalyst.

catalyzed by HCl and AuCl_3 to generate VCM. In contrast, if the HCl molecules could not be successfully adsorbed on the Au active sites, the chlorovinyl intermediate could not be desorbed readily from the AuCl_3 catalyst, which caused the side reaction and led to the rapid deactivation of the AuCl_3 due to the loss of Cl atoms [56]. Based on the above, we know that the adsorption of HCl has a strong influence on the stability of the AuCl_3 catalyst. For one thing, the adsorption of HCl is beneficial for improving the catalytic activity. For another, HCl can maintain the oxidative state of Au and inhibit the reduction of the active Au^{3+} species by C_2H_2 . Thus, the electron transfer from CuCl_2 molecule to AuCl_3 molecule, which stabilizes the catalytically active cationic Au species, is likely one of the reasons for the very high activity and stability of Au-Cu-IL/AC catalysts toward acetylene hydrochlorination. However, the activity enhancement is not exclusively a result of the electronic effect. A recent study using metal (Au, Pd, and Pt) nanoparticles/surfactant IL system for the catalytic hydrochlorination of acetylene suggested that anionic surfactant carboxylate ILs (ASC-ILs) had the feature of strong hydrogen-bond basicity (β), which was effective in absorbing and activating acetylene and HCl and thus contributing to enhanced activity [57]. The type of imidazolium chloride ionic liquid used in this study also has strong hydrogen-bond basicity and the β values reached almost 1.0 [58], so it is also expected to exhibit good absorption capacity for HCl and C_2H_2 . Thus, the physicochemical properties of IL may also exert a positive effect on the Au-Cu-IL/AC catalytic performance. In addition, the increase in activity seen here is directly associated with increase in the fraction of cationic Au species present in the catalysts. This could be determined from the XPS results of Au-Cu-IL/AC catalysts as shown in Figs. 3a and 7. Therefore, CuCl_2 additives may have a dual role. On the basis of the above analysis, we proposed a coupled redox cycle involving Cu^{2+} species (Scheme 2) to explain the stabilization of the Au^{3+} species. At this point, we considered that the successful application of the Wacker process relies on its ingenious catalytic cycle, in which the reduced Pd^0 is re-oxidized *in situ* to the active Pd^{2+} by Cu^{2+} [59–61]. Although, based on the redox potentials [62], it appears that the oxidation of metallic Au^0 by Cu^{2+} to cationic Au species (Au^{3+} and/or Au^+) might be difficult to achieve, it should be considered that the strong complexing ability of Cl^- present in the IL toward cationic Au species causes the redox potential from Au^0 to cationic Au species to be much lower, when compared to the redox potential without the abundant Cl^- [63]. The redox potentials for the Au^{3+} species are reported as follows [63]:

$$\text{Au}^{3+} + 3e^- = \text{Au}E^0 = 1.52 \text{ V}, \quad (1)$$

$$\text{AuCl}_4^- + 3e^- = \text{Au} + 4\text{Cl}^- E^0 = 1.00 \text{ V}. \quad (2)$$

Indeed, the reduction potential of Au^{3+} highly depends upon its coordination state and dramatic changes in the reduction potential are observed when Au^{3+} is coordinated with different atoms such as N, S, or Cl [64–67]. In addition, Cu^0 is easily re-oxidized to Cu^+ by HCl to form CuCl compound [68]. The formed CuCl is unstable in solution with respect to disproportionation into metallic Cu^0 and

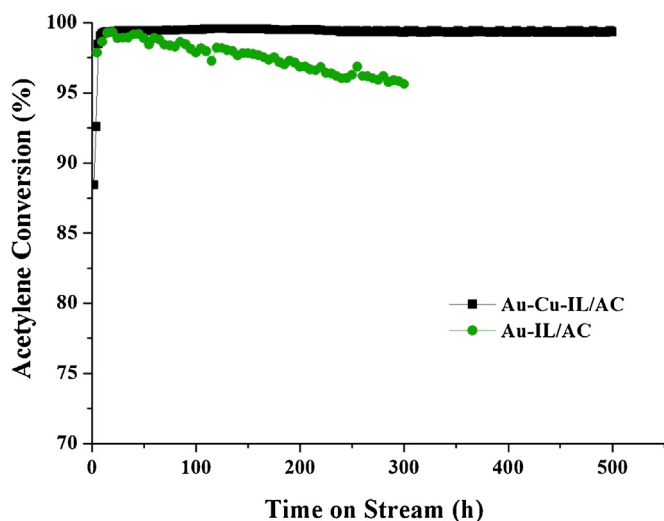


Fig. 10. Long-term stability test of Au-Cu-IL/AC catalyst. Reaction conditions: $T = 180^\circ\text{C}$, GHSV (C_2H_2) = 50 h^{-1} , feed volume ratio $V(\text{HCl})/V(\text{C}_2\text{H}_2) = 1.2:1$.

CuCl_2 to complete the catalytic cycle [69]. This novel synergistic effect between CuCl_2 and Au species provides a more efficient catalyst system for acetylene hydrochlorination to VCM than using the reported bimetallic Au-Cu/C catalysts [21,44–47].

3.6. Long-term stability of Au-Cu-IL/AC catalyst

In an attempt to further evaluate the long-term stability of the developed catalyst, we used the Au-Cu-IL/AC catalyst for 500 h time-on-stream under industrial conditions, as shown in Fig. 10. It was found that the catalytic activity did not drop significantly during 500 h of testing. A C_2H_2 conversion of 98.5% was achieved (total turnover number (tTON) is about 4.39×10^5 after running for 500 h) along with a 99.8% selectivity for VCM, indicating the high stability of the catalyst material. Moreover, in a previous work, the long-term stability test over the Au-IL/AC catalyst showed that the C_2H_2 conversion dropped significantly during a 300 h evaluation period [29]. This highlights the important role of CuCl_2 to stabilize cationic Au species during the hydrochlorination of acetylene. Evidently, the Au-Cu-IL/AC is stable under typical reaction conditions for acetylene hydrochlorination.

4. Conclusions

Exploration of the unique catalytic abilities of Au^{3+} species has been hampered by difficulties in accessing the higher oxidation state and the challenges associated with stabilizing them during preparation and use. In this work, CuCl_2 has been introduced as a modifier of the Au-SILP catalytic system and the modified Au-Cu-IL/AC was evaluated in the hydrochlorination of acetylene. The catalyst based on Au-Cu-IL exhibited $>72.1\%$ C_2H_2 conversion ($\text{TOF} = 168.5 \text{ h}^{-1}$), which is 1.8 times that of the non-promoted catalyst and by far exceeds the best performance of all Au-based catalyst systems reported in the literature. The Au-Cu-IL/AC catalyst also displayed stable performance with only negligible conversion loss under the typical industrial acetylene hydrochlorination reaction conditions even after 500 h of operation. Based on BET, XRD, TEM, XPS, ICP-MS and TGA analyses, it is proposed that the enhanced catalytic performance is due to inhibition of the reduction of cationic Au species by addition of Cu^{2+} to re-oxidize the reduced Au^0 as well as the electronic interaction between gold and copper species. The present results might bring light to new opportuni-

ties in developing high-efficiency cationic gold-based catalysts by the introduction of oxidant components into the catalysts.

Acknowledgements

Financial support from the National Natural Science Foundation of China (NSFC; grant Nos. 21606199, 21303163, 21476207) and the China Postdoctoral Science Foundation (No. 2016M592015) are gratefully acknowledged.

References

- [1] H. Schobert, Chem. Rev. 114 (2014) 1743–1760.
- [2] M.Y. Zhu, Q.Q. Wang, K. Chen, Y. Wang, C.F. Huang, H. Dai, F. Yu, L.H. Kang, B. Dai, ACS Catal. 5 (2015) 5306–5316.
- [3] G.J. Hutchings, D.T. Grady, Appl. Catal. 16 (1985) 411–415.
- [4] P. Johnston, N. Carthey, G.J. Hutchings, J. Am. Chem. Soc. 137 (2015) 14548–14557.
- [5] G.J. Hutchings, D.T. Grady, J. Catal. 96 (1985) 292–295.
- [6] M. Conte, A.F. Carley, G.J. Hutchings, Catal. Lett. 124 (2008) 165–167.
- [7] S.A. Mitchenko, T.V. Krasnyakova, R.S. Mitchenko, A.N. Korduban, J. Mol. Catal. A: Chem. 275 (2007) 101–108.
- [8] T.V. Krasnyakova, I.V. Zhikharev, R.S. Mitchenko, V.I. Burkhevetski, A.M. Korduban, T.V. Kryshchuk, S.A. Mitchenko, J. Catal. 288 (2012) 33–43.
- [9] L. Wang, F. Wang, J.D. Wang, Catal. Commun. 65 (2015) 41–45.
- [10] Y.F. Pu, J.L. Zhang, L. Yu, Y.H. Jin, W. Li, Appl. Catal. A: Gen. 488 (2014) 28–36.
- [11] J.T. Xu, J. Zhao, T.T. Zhang, X.X. Di, S.C. Gu, J. Ni, X.N. Li, RSC Adv. 5 (2015) 38159–38163.
- [12] K. Zhou, J.K. Si, J.C. Jia, J.Q. Huang, J. Zhou, G.H. Luo, F. Wei, RSC Adv. 4 (2014) 7766–7769.
- [13] K. Zhou, J.C. Jia, X.G. Li, X.D. Pang, C.H. Li, J. Zhou, G.H. Luo, F. Wei, Fuel Process. Technol. 108 (2013) 12–18.
- [14] K. Zhou, B. Li, Q. Zhang, J.Q. Huang, G.L. Tian, J.C. Jia, M.Q. Zhao, G.H. Luo, D.S. Su, F. Wei, ChemSusChem 7 (2014) 723–728.
- [15] X.Y. Li, X.L. Pan, L. Yu, P.J. Ren, X. Wu, L.T. Sun, F. Jiao, X.H. Bao, Nat. Commun. 5 (2014) 3688–3674.
- [16] H.Y. Zhang, W. Li, Y.H. Jin, W. Sheng, M.C. Hui, X.Q. Wang, J.L. Zhang, Appl. Catal. B: Environ. 189 (2016) 56–64.
- [17] B. Nkosi, N.J. Coville, G.J. Hutchings, M.D. Adams, J. Friedl, F.E. Wagner, J. Catal. 128 (1991) 366–377.
- [18] J.L. Zhang, Z.H. He, W. Li, Y. Han, RSC Adv. 2 (2012) 4814–4821.
- [19] M. Conte, A.F. Carley, G. Attard, A.A. Herzing, C.J. Kiely, G.J. Hutchings, J. Catal. 257 (2008) 190–198.
- [20] H.Y. Zhang, B. Dai, X.G. Wang, L.L. Xu, M.Y. Zhu, J. Ind. Eng. Chem. 18 (2012) 49–54.
- [21] S.J. Wang, B.X. Shen, Q.L. Song, Catal. Lett. 134 (2010) 102–109.
- [22] K. Zhou, W. Wang, Z. Zhao, G.H. Luo, J.T. Miller, M.S. Wong, F. Wei, ACS Catal. 4 (2014) 3112–3116.
- [23] H.Y. Zhang, B. Dai, X.G. Wang, W. Li, Y. Han, J.J. Gu, J.L. Zhang, Green Chem. 15 (2013) 829–836.
- [24] J. Zhao, J.T. Xu, J.H. Xu, J. Ni, T.T. Zhang, X.L. Xu, X.N. Li, ChemPlusChem 80 (2015) 196–201.
- [25] G.B. Li, W. Li, J.L. Zhang, Catal. Sci. Technol. 6 (2016) 3230–3237.
- [26] X.Y. Li, M.Y. Zhu, B. Dai, Appl. Catal. B: Environ. 142 (2013) 234–240.
- [27] J. Zhao, J.T. Xu, J.H. Xu, T.T. Zhang, X.X. Di, J. Ni, X.N. Li, Chem. Eng. J. 262 (2015) 1152–1160.
- [28] B.G. Wang, L. Yu, J.L. Zhang, Y.F. Pu, H.Y. Zhang, W. Li, RSC Adv. 4 (2014) 15877–15885.
- [29] J. Zhao, S.C. Gu, X.L. Xu, T.T. Zhang, Y. Yu, X.X. Di, J. Ni, Z.Y. Pan, X.N. Li, Catal. Sci. Technol. 6 (2016) 3263–3270.
- [30] C.P. Mehnert, R.A. Cook, N.C. Dispenziere, M. Afeworki, J. Am. Chem. Soc. 124 (2002) 12932–12933.
- [31] F. Schwab, M. Lucas, P. Claus, Angew. Chem. Int. Ed. 50 (2011) 10453–10456.
- [32] S. Werner, N. Sznesi, R.W. Fischer, M. Haumann, P. Wasserscheid, Phys. Chem. Chem. Phys. 11 (2009) 10817–10819.
- [33] M. Haumann, K. Dentler, J. Joni, A. Riisager, P. Wasserscheid, Adv. Synth. Catal. 349 (2007) 425–431.
- [34] L.F. Bobadilla, T. Blasco, J.A. Odriozola, Phys. Chem. Chem. Phys. 15 (2013) 16927–16934.
- [35] Q.Q. Zhu, S. Maeno, M. Sasaki, T. Miyamoto, M. Fukushima, Appl. Catal. B: Environ. 163 (2015) 459–466.
- [36] M. Paszkiewicz, J. Luczak, W. Lisowski, P. Patyk, A. Zaleska-Medynska, Appl. Catal. B: Environ. 184 (2016) 223–237.
- [37] H.S. Schrekker, M.A. Gelesky, M.P. Stracke, C.M. Schrekker, G. Machado, S.R. Teixeira, J.C. Rubim, J. Dupont, J. Colloid Interface Sci. 316 (2007) 189–195.
- [38] P. Mierczynski, K. Vasilev, A. Mierczynska, W. Maniukiewicz, M.I. Szynkowska, T.P. Maniecki, Appl. Catal. B: Environ. 185 (2016) 281–294.
- [39] N.K. Gamboa-Rosales, J.L. Ayastuy, Z. Boukha, N. Bion, D. Duprez, J.A. Pérez-Omil, E. del Río, M.A. Gutiérrez-Ortiz, Appl. Catal. B: Environ. 168–169 (2015) 87–97.
- [40] A. Sandoval, C. Louis, R. Zanella, Appl. Catal. B: Environ. 140–141 (2013) 363–377.
- [41] S.A. Nikolaev, E.V. Golubina, I.N. Krotova, M.I. Shilina, A.V. Chistyakov, V.V. Kriventsov, Appl. Catal. B: Environ. 168–169 (2015) 303–312.
- [42] T.R. Reina, S. Ivanova, M.A. Centeno, J.A. Odriozola, Appl. Catal. B: Environ. 187 (2016) 98–107.
- [43] X. Liao, W. Chu, X. Dai, V. Pitchon, Appl. Catal. B: Environ. 142–143 (2013) 25–37.
- [44] J.M. Ma, S.J. Wang, B.X. Shen, React. Kinet. Mech. Catal. 110 (2013) 177–186.
- [45] H. Xu, K. Zhou, J.K. Si, C.H. Li, G.H. Luo, Catal. Sci. Technol. 6 (2016) 1357–1366.
- [46] J. Zhao, S.C. Gu, X.L. Xu, T.T. Zhang, X.X. Di, Z.Y. Pan, X.N. Li, RSC Adv. 5 (2015) 101427–101436.
- [47] H.Y. Zhang, B. Dai, W. Li, X.G. Wang, J.L. Zhang, M.Y. Zhu, J.J. Gu, J. Catal. 316 (2014) 141–148.
- [48] P. Moriel, A.B. García, Green Chem. 16 (2014) 4306–4311.
- [49] F. Neațu, V.I. Părvulescu, V. Michelet, J.P. Génét, A. Goguet, C. Hardacre, New J. Chem. 33 (2009) 102–106.
- [50] M. Conte, C.J. Davies, D.J. Morgan, A.F. Carley, P. Johnston, G.J. Hutchings, Catal. Lett. 144 (2014) 1–8.
- [51] F. Severino, J.L. Brito, J. Laine, J.L.G. Fierro, A.L. Agudo, J. Catal. 177 (1998) 82–95.
- [52] I. Platzman, R. Brener, H. Haick, R. Tannenbaum, J. Phys. Chem. C 112 (2008) 1101–1108.
- [53] M. Conte, C.J. Davies, D.J. Morgan, T.E. Davies, D.J. Elias, A.F. Carley, P. Johnston, G.J. Hutchings, J. Catal. 297 (2013) 128–136.
- [54] Y.Y. Fong, B.R. Visser, J.R. Gascooke, B.C.C. Cowie, L. Thomsen, G.F. Metha, M.A. Buntine, H.H. Harris, Langmuir 27 (2011) 8099–8104.
- [55] Y.X. Ding, Y.X. Sun, L.Y. Zhang, S.J. Mao, Z.L. Xie, Z.W. Liu, D.S. Su, Angew. Chem. Int. Ed. 54 (2015) 231–235.
- [56] J.L. Zhang, Z.H. He, W. Li, Y. Han, RSC Adv. 2 (2012) 4814–4821.
- [57] J.Y. Hu, Q.W. Yang, L.F. Yang, Z.G. Zhang, B.G. Su, Z.B. Bao, Q.L. Ren, H.B. Xing, S. Dai, ACS Catal. 5 (2015) 6724–6731.
- [58] C. Chiappe, C.S. Pomelli, S. Rajamani, J. Phys. Chem. B. 115 (2011) 9653–9661.
- [59] J.E. Backvall, B. Åkermark, S.O. Ljunggren, J. Am. Chem. Soc. 101 (1979) 2411–2416.
- [60] J. Smidt, W. Hafner, R. Jira, R. Sieber, R. Ruttinger, H. Kojer, Angew. Chem. 71 (1959) 176–182.
- [61] J.A. Keith, R.J. Nielsen, J. Osgaard, W.A. Goddard, J. Am. Chem. Soc. 129 (2007) 12342–12343.
- [62] L.C. Cox, Appl. Organometal. Chem. 17 (2003) 79.
- [63] A.J. Bard, R. Parsons, J. Jordan, Standard Potentials in Aqueous Solution, Marcel Dekker Inc, New York, 1985.
- [64] M. Hojo, Y. Uji-yie, S. Tsubota, M. Tamura, M. Yamamoto, K. Okamura, K. Isshiki, J. Mol. Liq. 194 (2014) 68–76.
- [65] M. Hojo, M. Yamamoto, K. Okamura, Phys. Chem. Chem. Phys. 17 (2015) 19948–19956.
- [66] K. Zhou, J.C. Jia, C.H. Li, H. Xu, J. Zhou, G.H. Luo, F. Wei, Green Chem. 17 (2015) 356–364.
- [67] C.Y. Wu, T. Horibe, C.B. Jacobsen, F.D. Toste, Nature 517 (2015) 449–454.
- [68] M.V. Twigg, M.S. Spencer, Top. Catal. 22 (2003) 191–203.
- [69] N.N. Greenwood, A. Earnshaw, Chemistry of the Elements, 2nd ed., Butterworth-Heinemann Oxford, UK, 1997.